Photoluminescence of Water-Soluble Conjugated Polymers: Origin of Enhanced Quenching by Charge Transfer

Jian Wang, Deli Wang, Edward K. Miller, Daniel Moses, Guillermo C. Bazan, and Alan J. Heeger*

Institute for Polymers and Organic Solids, University of California at Santa Barbara, Santa Barbara, California 93106-5090

Received January 19, 2000; Revised Manuscript Received April 18, 2000

ABSTRACT: Quenching of the photoluminescence (PL) emission from conjugated macromolecules by charge transfer to cationic electron acceptors is studied by changing the ion concentration in buffered aqueous solutions, by changing the concentration of acceptors, and by varying the temperature. A weakly bound complex is formed (in water) between polyanionic conjugated macromolecules and cationic electron acceptors with Coulomb binding energy ∼150 meV. The mean distance between the polymer$^{(-)}$ and quencher$^{(+)}$ was estimated as 10 Å, consistent with the effective charge-transfer distance. At high quencher concentrations, quenching by acceptors within the sphere-of-action becomes important; a modified Stern−Volmer equation is used to estimate the radius (∼400 Å). High-temperature studies of concentrated quencher solutions independently indicate a crossover from static quenching to sphere-of-action quenching with a radius ∼400 Å. Since the radius is comparable to the radius of gyration of the macromolecule, the high molecular weight of the conjugated polymer enhances the quenching.

Introduction

Research on the optoelectronic properties of conjugated (semiconducting) polymers has created opportunities for a number of applications, such as light-emitting diodes,[1] light-emitting electrochemical cells,[2] solid-state lasers,[3] solar cells,[4] and photodetectors.[5] The recent discovery of more than a millionfold amplification of the sensitivity to fluorescence quenching by Chen et al.[6] opens an opportunity for conjugated polymers in biological and chemical sensors for use in medical diagnostics and toxicology.

Poly(phenylenevinylene), PPV, and its various derivatives are among the most studied conjugated polymers, since they are known to exhibit photoluminescence (PL) with high quantum efficiency.[7] By attaching functional side groups onto the conjugated backbone, these macromolecules can be made soluble in common organic solvents or in water. Typical molecular weights are on the order of 10^6 Da, corresponding to approximately 500−1000 monomer repeat units per macromolecule.

The fundamental scientific discovery by Chen et al. is that the PL of a negatively charged PPV derivative in aqueous solution is quenched via photoinduced electron transfer. By using low concentrations of the cationic electron acceptor, methyl viologen (MV^{2+}), Chen et al. showed that a single MV^{2+} quenches the PL from approximately 1000 repeat units; i.e., one MV^{2+} quenches the PL from an entire macromolecule. This remarkable enhancement in the PL quenching was used to demonstrate the potential for creating a new class of high-sensitivity biosensors. By connecting the quencher (MV^{2+}) to a biologically interesting ligand (biotin) through a flexible tether, Chen and colleagues demonstrated that the fluorescence is fully recovered upon binding between the biotin and the specific analyte protein, avidin; the biotin−avidin complex pulls the MV^{2+} away from the PPV chain and thereby shuts down the photoinduced electron transfer. The polymer-based biosensor approach has the potential to be a significant improvement over current standard technologies.[8]

The enhanced fluorescence quenching observed for the PPV:MV^{2+} system (with $LiSO_3$ terminal groups on the side chains of the PPV derivative; see Figure 1) arises from a combination of two effects. First, as noted above, from the concentrations used in the experiments it appears that a single MV^{2+} molecule can quench the fluorescence emission from an entire macromolecule. Second, in aqueous solution, there is an equilibrium

$$-SO_3^-Li^+ \Leftrightarrow -SO_3^- + Li^+ \qquad (1)$$

such that the luminescent polymer is negatively charged (anionic). As a result, the positively charged acceptor and the anionic polymer form a weakly bound complex, thereby significantly enhancing the local concentration of the quencher molecules in the proximity of the luminescent polymer. Thus, determining the magnitude of the Coulomb binding energy of the polymer:quencher complex is of particular importance. If the binding between the ligand tethered to the quencher and the analyte protein is smaller than that between the quencher and the polymer, the quencher/ligand cannot be effectively pulled away from the luminescent polymer. This last point is particularly relevant to the studies by Chen et al. in that the detected "unquenching" of fluorescence was likely due, in part, to steric effects, i.e., the large size of the avidin prevented avidin-bound quencher/biotin from interacting with the polymer.

The details of the quenching mechanism have not yet been clarified. We expect static quenching by complex formation to dominate at low quencher concentrations. Because of the high molecular weight of the macromolecule (and hence the relatively large radius of gyration) and the enhanced local concentration of the quencher, quenching within a sphere-of-action will become important at high quencher concentrations.

In this article, we address the mechanism for enhanced quenching through a comprehensive study of the

* Corresponding author. E-mail ajh@physics.ucsb.edu.

10.1021/ma000081j CCC: $19.00
Published on Web 06/17/2000

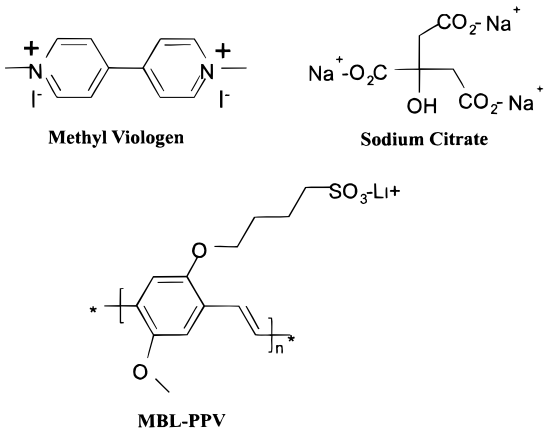

Figure 1. Chemical structure of MBL−PPV, MV^{2+}, and sodium citrate.

effect of temperature on the PL of poly[5-methoxy-2-(4-sulfobutoxy)-1,4-phenylenevinylene], MBL−PPV, with MV^{2+} in pure water and in buffered water. From the temperature profile of the PL quenching data, and by changing the ion concentration (and thereby the Debye screening length) in the buffered solutions, we identify the basic quenching mode to be static via formation of a bound complex, and we obtain information on the magnitude of the binding energy of the complex. Studies at high quencher concentrations in pure water provide information on the sphere-of-action quenching.

The Debye screening length is used to characterize the buffered solutions. The mean distance and binding energy between polymer and quencher are derived from a comparison of the data with calculations of the screening length and binding energy. The binding energy is estimated to be approximately 150 meV, and the mean distance is approximately 10 Å.

From the data obtained at high quencher concentrations, we estimate the radius of the sphere-of-action to be about 400 Å, comparable to the end-to-end dimension of the polymer chain. Thus, the relatively high molecular weight of the conjugated polymer enhances the quenching.

Experimental Methods

Materials. MBL−PPV was synthesized following the published procedure,[9] except that the monomer, 2-methoxy-5-butyloxysulfonate sodium, was made by reacting 4-methoxyphenol with 1,4-butane sultone under base conditions. Methyl viologen (MV^{2+}) was synthesized from iodomethane and 4,4′-dipyridyl in dry DMF. The water used in making the stock solution of MBL−PPV and MV^{2+} was purged with nitrogen for at least 4 h immediately prior to usage. The stock solution (defined as $20c_0$, i.e., 20-fold) of sodium chloride sodium citrate (SSC) buffer (3 M of NaCl and 0.3 M of sodium citrate, pH = 7) was made using nano-pure water. At $1c_0$, the salt concentrations are 0.15 M NaCl and 0.015 M sodium citrate, pH = 7.

The solutions used in the temperature studies, in pure water, or in buffered water with different concentrations were made by taking the calculated amount of the stock solution and diluting to the concentrations needed using freshly N_2-purged water. All chemicals were obtained from Fisher Scientific Co. or Aldrich Chemical Co. and were used as received. The chemical structures of MBL−PPV, MV^{2+}, and sodium citrate are illustrated in Figure 1.

Instrumentation. The 457.9 nm emission line from an argon laser was used as excitation source. The light intensity was adjusted to obtain enough signal without damaging the material. Phase-sensitive detection and a photomultiplier tube were employed to measure the PL from the sample. To correct for any the error introduced by fluctuations of the light source, a reference beam was split from the excitation beam and measured at the same time as that of PL signal. By normalizing the PL data to the reference reading, an error less than 1% was achieved. Temperature was read by a silicon diode connected to temperature controller (Scientific Instrument). The temperature-dependent PL data were taken from room temperature to high temperature (e.g., 75 °C) and then back to room temperature in order to verify the reproducibility of the data. No hysteresis was observed.

Results and Discussion

Debye Length. In an electrolyte, the Coulomb interaction is screened by the free ions and decreases with distance faster than the inverse distance dependence. In first-order approximation, the Coulomb potential exhibits an exponential decay and takes the following form[10]

$$\phi \approx \phi_0 e^{-\kappa x} \tag{2}$$

where ϕ_0 is the surface potential of a charged plane located at $x = 0$, and

$$\frac{1}{\kappa} = \sqrt{\frac{\epsilon kT}{\sum_i \rho_{\infty i} q_i^2}} \tag{3}$$

is defined as the Debye length. Because the magnitude of the Debye length depends solely on the properties of the electrolyte, it is a characteristic measure of ionic screening. In the above definition of the Debye length, $\rho_{\infty i}$ is the ionic concentration of ions i in the bulk (at $x = \infty$), q_i is the charge of ions i, ϵ is the dielectric constant of the electrolyte, k is the Boltzmann constant, and T is the temperature. The surface potential ϕ_0 is related to the surface charge density, σ, by Gauss's law:

$$\sigma = -\frac{1}{2}\epsilon\left(\frac{d\phi}{dx}\right)_{x=0} = \epsilon\kappa\phi_0 \tag{4}$$

If the surface charge density and the concentration of the electrolyte are known, one can determine the binding energy between an ion and the charged surface. Assuming that the charge of the ion is Q and that the charge is located at approximately one Debye length from the surface, the binding energy is

$$W = Q\phi_{1/\kappa} = Q\phi_0 e^{-1} \tag{5}$$

Binding Energy of MBL−PPV:MV^{2+} Complex in SSC Buffer. Figure 2 illustrates the SSC buffer concentration dependence of the PL from MBL−PPV and from the MBL−PPV:MV^{2+} complex at room temperature. The PL from pure MBL−PPV is not affected by the ion concentration. The PL from MBL−PPV in the MBL−PPV:MV^{2+} complex is fully recovered in the concentrated buffer solution, since the buffer ions screen the Coulomb interaction and thereby remove the MV^{2+} from the vicinity of the polymer. The transition from quenched (off) state to unquenched (on) state as the buffer concentration is increased is clearly shown. This transition indicates a static quenching mechanism for the MBL−PPV:MV^{2+} system. Dynamic quenching would not be affected by the buffer ions.

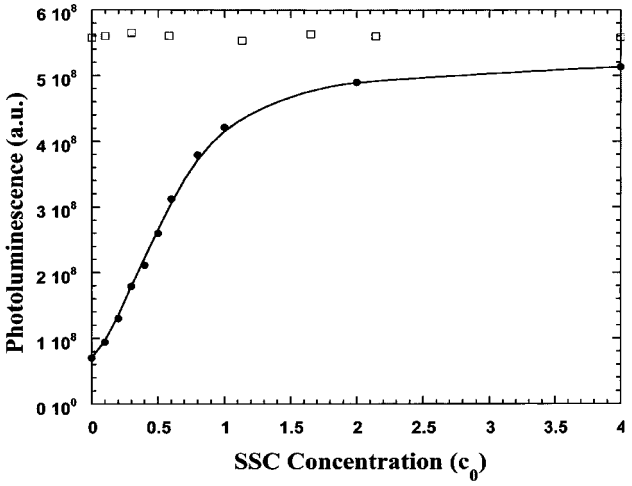

Figure 2. Photoluminescence from MBL−PPV (empty squares) and MBL−PPV:MV^{2+} (solid circles) versus the concentration of the SSC buffer. The solid line is the smooth fit of the PL from the complex. The concentration of MBL−PPV is 1×10^{-5} M, and that of MV^{2+} is 4×10^{-7} M. The buffer concentration is in units of c_0: $1c_0$ SSC buffer contains 0.15 M NaCl and 0.015 M sodium citrate, pH = 7.

Table 1. Comparison of the Binding Energy Derived from Debye Length and the Binding Energy from the Data Fitting

SSC concn[a]	Debye length (Å)	binding energy at Debye length (meV)	fitted binding energy (meV)
0.2	14.6	219	103
0.3	11.4	171	77
0.5	8.79	132	46
1	6.22	93.3	40
2	4.4	66	39
4	3.11	46.7	25

[a] The units of buffer's concentration is in c_0 (fold). $1c_0$ SSC contains 0.15 M NaCl and 0.015 M sodium citrate, pH = 7.

The Debye length and the binding energy at the Debye length in different buffer concentrations are obtained by using eqs 3−5. The surface charge density σ of the polymer is derived by assuming one electron charge per area of the repeat unit; the actual charge density might be somewhat lower (see eq 1). The results are summarized in Table 1.

The binding energy decreases when the ion concentration is increased. By taking the derivative of the PL with respect to the buffer concentration, one finds the concentration which causes the sharpest change. Figure 3 shows the slope as a function of the buffer concentration. The maximum slope occurs at the concentration of $0.3c_0$ (0.045 M NaCl and 0.0045 M sodium citrate, pH = 7). At this concentration, the Debye screening length is comparable to the distance between the MBL−PPV and MV^{2+}. Thus, the mean distance between MBL−PPV and MV^{2+} is estimated to be around 10 Å, and the binding energy of the complex in pure water is approximately 150 meV. Note that since the distance for effective charge transfer is approximately 10 Å, the binding energy of the MBL−PPV:MV^{2+} complex is nearly optimized for sensitivity in the biosensor application.

At high temperatures, for static quenching, thermal fluctuations will tend to dissociate the MV^{2+} from MBL−PPV. Thus, the quenched fluorescence is expected to increase at high temperature. Figure 4 illustrates the change with temperature of PL from the complex and from the pure polymer in $0.2c_0$ (0.03 M NaCl and 0.003 M sodium citrate, pH = 7) buffer solution. The temperature profile of the PL clearly shows that the basic quenching mode is static. To show the change of PL more clearly, the data at high temperature are normalized to the value at room temperature. The PL from pure MBL−PPV decreases with increasing temperature indicative of an increase in the probability for nonradiative decay via thermal fluctuations. To compensate for this intrinsic decrease, the PL from the complex is normalized to the data from the pure polymer. As the ion concentration increases and the binding energy between MBL−PPV and MV^{2+} decreases, thermal fluctuations are more effective in dissociating the complex. Thus, the increase of PL relative to that at room temperature should be larger in the more concentrated buffer. However, at high buffer concentrations, where the PL is already recovered at room temperature, increasing the temperature will have little effect. Therefore, the increase of PL relative to that at room temperature should be smaller. The largest increase should occur at the same concentration at which the binding energy of the complex is screened, i.e., at approximately $0.3c_0$ (0.045 M NaCl and 0.0045 M sodium citrate, pH = 7). Figure 5 shows the relative PL increase at 75 °C versus the buffer concentration. The peak is located at $0.2c_0$ (0.03 M NaCl and 0.003 M sodium citrate, pH = 7), roughly consistent with the data in Figure 3.

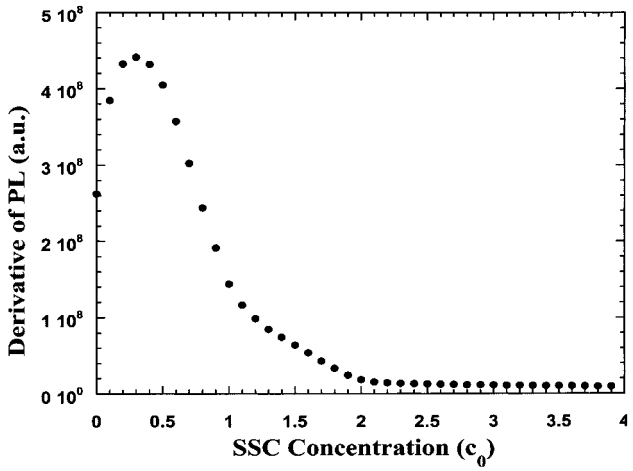

Figure 3. Derivative of smooth fitted PL from MBL−PPV:MV^{2+} with respect to the buffer concentration.

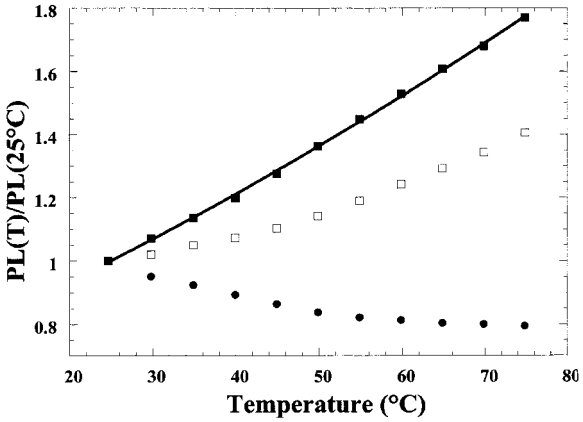

Figure 4. Photoluminescence relative to that at room temperature from MBL−PPV (solid circles) and MBL−PPV:MV^{2+} (empty squares) versus the temperature. The solid squares are the PL from the complex normalized to that from the pure polymer. The fit by eq 5 is plotted as the solid line.

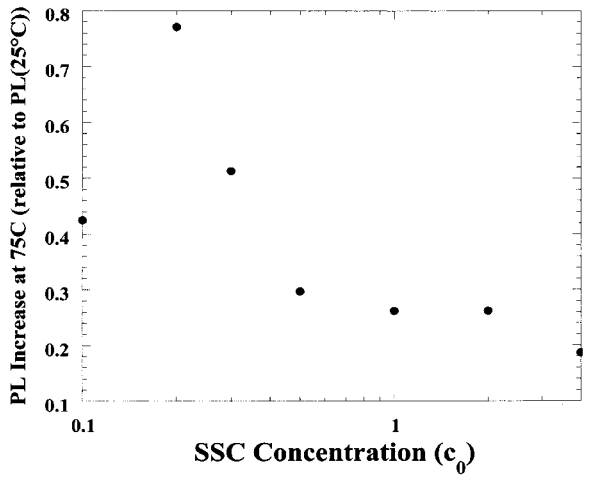

Figure 5. Relative PL increase at 75 °C versus the buffer concentration.

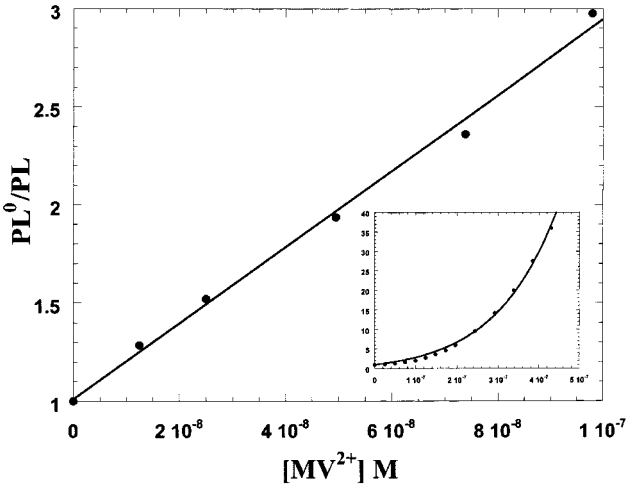

Figure 6. Stern−Volmer plot (PL of MBL−PPV at 1×10^{-5} M over the PL of polymer with MV^{2+} versus the MV^{2+} concentration) from 1×10^{-8} to 1×10^{-7} M. Inset: the same plot extended to higher MV^{2+} concentrations (from 1×10^{-8} to 4.3×10^{-7} M). The solid line is the fit obtained from the modified Stern−Volmer equation.

To find the binding energy from the temperature-dependent PL data, we fit the data as a simple, temperature-activated process:

$$PL(T) = PL_0 e^{-W/kT} \tag{6}$$

where W is the binding energy. The best fit values for binding energies at different buffer concentrations are shown in Table 1.

Considering the many assumptions in the derivation of Debye screening length and the simple function used to fit the data, the values obtained from the fits are in agreement with the values derived from the Debye length. The trends are certainly correct. The absolute values can be brought into excellent agreement if one assumes a charge density of $0.5e$ per repeat unit (see eq 1). At a buffer concentration of $4c_0$ (0.6 M NaCl and 0.06 M sodium citrate, pH = 7), the binding energy of the complex is only about 25 meV, i.e., comparable to the thermal energy at room temperature. As shown in Figure 2, the fluorescence is fully recovered at this concentration at room temperature.

Sphere-of-Action Quenching of MBL−PPV. There are two general types of quenching:[11] (1) static quenching through the formation of a complex; (2) dynamic quenching due to random collisions between the PL emitter and the acceptor. Both processes can be quantitatively described by the Stern−Volmer equation:

$$\frac{PL^0}{PL} = 1 + K_{SV}[\text{quencher}] \tag{7}$$

where the PL^0 is the intensity of fluorescence in the absence of the quencher and PL is the intensity of fluorescence in the presence of the quencher. The Stern−Volmer constant, K_{SV}, provides a quantitative measure of the quenching. The extremely large Stern−Volmer constant (1.9×10^7 M^{-1}) found in the MBL−PPV:MV^{2+} system is primarily the result of static quenching through the formation of a bound complex, i.e., static quenching (as discussed in the previous section and elsewhere).[6,8] In static quenching, the Stern−Volmer constant is the association constant for complex formation,[12] which is

$$K_{SV}^S = \frac{[FQ]}{[F][Q]} \tag{8}$$

where [FQ], [F], and [Q] are the concentrations of complex, fluorophore, and quencher, respectively. From the above equation, it is straightforward to calculate the probability (f) that a fluorophore is not complexed:[12]

$$f = \frac{[F]}{[F] + [FQ]} = \frac{1}{1 + K_{SV}^S[Q]} = \frac{PL}{PL^0} \tag{9}$$

Figure 6 illustrates the PL^0/PL versus the quencher concentration. At low concentrations, PL^0/PL increases linearly with the quencher concentration. By fitting the data with linear equation, the Stern−Volmer constant at low concentrations is found to be 1.9×10^7 M^{-1}.

As the concentration increases, superlinear behavior appears as shown in the inset of Figure 6, implying the onset of an additional quenching mechanism. To account for this positive deviation from the linear curve, the concept of a "sphere-of-action" was introduced into the Stern−Volmer equation by Frank and Vavilov.[13] In the polymer$^{(-)}$:quencher$^{(+)}$ system, since the local concentration of the quencher is enhanced by the tendency toward complex formation, an additional factor α is also introduced.[14] At high quencher concentration ($\sim 2 \times 10^{-5}$ M), the MV^{2+} molecules have a mean separation of only about 800 Å. Considering the large size of the conjugated polymer in aqueous solution, in this high concentration regime, there are always quencher molecules within a charge transfer distance from one of the conjugated macromolecules; i.e., there are always quenchers within the sphere-of-action of the polymer. In this regime, the quenching is expected to increase superlinearly with the quencher concentration.

The probability (f') of finding a fluorophore without any quencher within the sphere-of-action is[12,13]

$$f' = e^{-vN[Q]} \tag{10}$$

where v is the volume of the sphere-of-action, N is Avogadro's number, and [Q] is the quencher concentration. Thus, the existence of the sphere-of-action reduces the proportion of uncomplexed fluorophores by another

factor $\exp(-vN[Q])$, which in turn reduces the fluorescence by the same factor:[18]

$$\frac{PL}{PL^0} = ff' = \frac{1}{1 + K_{SV}^S[Q]} e^{-vN[Q]} \quad (11)$$

Upon rearrangement, the above equation becomes

$$\frac{PL^0}{PL} = (1 + K_{SV}^S[Q])e^{vN[Q]} = (1 + K_{SV}^S[Q])e^{\alpha V[Q]} \quad (12)$$

where volume constant V is defined as vN,[15] and α is introduced to account for the charge-induced enhancement of the local quencher concentration.[14] This modified form of the Stern−Volmer equation describes the combination of static quenching plus dynamic quenching within the sphere-of-action (Figure 6).

From the best fit of eq 12 to the data at high quencher concentrations (keeping only the leading term of the exponential), the static Stern−Volmer constant was found to be 1.9×10^7 M^{-1} as same as that one obtained at low concentration regime by linear fit, and the product αV was found to be 4.8×10^6 M^{-1}. The volume constant $\sim 2 \times 10^5$ M^{-1}, corresponding to a sphere-of-action with radius ~400 Å, is obtained from similar data using a neutral 4,4′-dipyridyl, Dpy, as the quencher, i.e., the MBL−PPV:Dpy system.[14] This length scale is consistent with the radius of gyration of the polymer in solution. Assuming a "random walk" conformation of the polymer chain, the size of the polymer is proportional to $\sqrt{N}a$,[17] where N is the number of repeat units (~1000) and a is the size of one repeat unit (~10 Å for MBL−PPV). Thus, the approximate hydrodynamic diameter of the polymer is

$$\sqrt{N}a \approx \sqrt{1000} \times 10 \text{ Å} \approx 320 \text{ Å}$$

The temperature dependence of the PL from MBL−PPV and MBL−PPV:MV^{2+} is illustrated in Figure 7. To show the change of PL more clearly, the PL data are normalized to the value at room temperature. The fluorescence from the pure polymer decreases with increasing temperature, similar to the trend in the buffered solution. For the complex, the PL increases at high temperature, as the thermal energy pulls the MV^{2+} away from MBL−PPV. As more quencher is added, while the absolute value of PL becomes lower (in Figure 6), the relative increase at 75 °C gets larger (in Figure 7a). At quencher concentrations above 1×10^{-5} M, the relative fluorescence increase at 75 °C starts to diminish, as shown clearly in Figure 8. The lower increase at high quencher concentration results from the sphere-of-action. As noted above, if a quencher is within the action sphere of the polymer, it will quench the fluorescence, giving rise to the exponential factor in the Stern−Volmer equation. While the static quenching leads to unquenching at high temperature through the dissociation of the complex, the concentrated quencher solution prevents the quencher from leaving the sphere-of-action of the polymer. The peak at 1×10^{-5} M concentration shows the transition from static quenching to sphere-of-action quenching.

At the crossover point, if we assume the MV^{2+} is uniformly distributed in the solution at high temperature, each MV^{2+} will occupy a volume of ~700 $Å^3$. Thus,

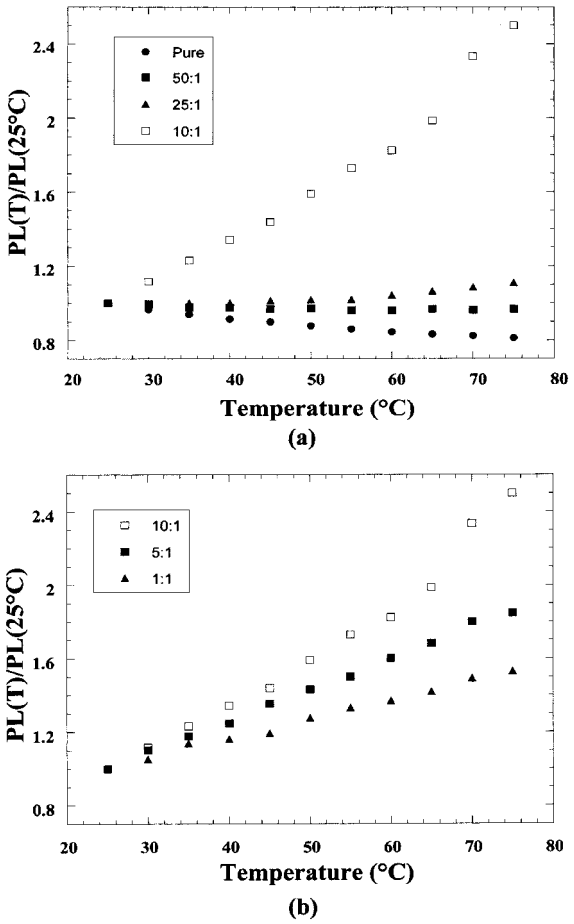

Figure 7. PL from MBL−PPV (solid circle) and MBL−PPV:MV^{2+} with different MV^{2+} concentration versus temperature. The MBL−PPV concentration is kept at 1×10^{-4} M. The concentration of MV^{2+} ranges from 1000:1 to 1:1 in units of the ratio of monomer number to MV^{2+} number.

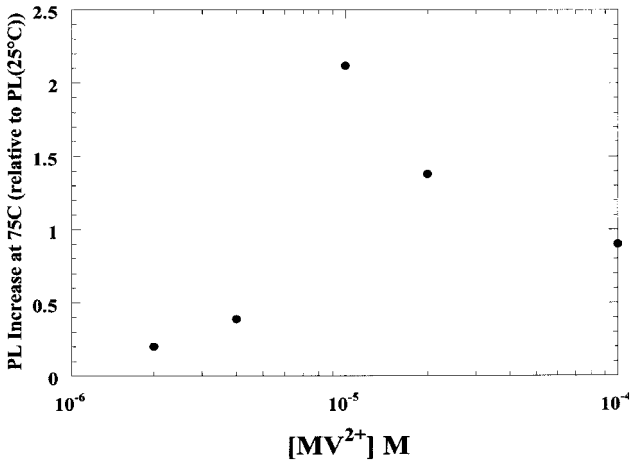

Figure 8. Relative PL increase of MBL−PPV:MV^{2+} versus the concentration of the MV^{2+}. The concentration of MBL−PPV is kept at 1×10^{-4} M.

within the sphere-of-action of MBL−PPV, there is at least one MV^{2+} present to quench the fluorescence from the polymer. This is another indication of the sphere-of action with a size that is the same as that obtained by fitting the data to the modified Stern−Volmer equation. As the quencher concentration is increased, there are more and more MV^{2+} ions within the sphere-of-action of the MBL−PPV. Thus, the relative PL increase at high temperature diminishes.

Conclusions

In buffered solutions, the ions screen the Coulomb interaction between the negatively charged polymer and the positively charged quencher. A transition from quenched state (off) to the unquenched state (on) is observed as a function of the ion concentration. The binding energy is calculated by using the Debye length, which is a characteristic measure of screening in ionic solutions. The critical concentration, obtained through two independent experiments, yields an estimate for the binding energy between MBL−PPV and MV^{2+} of ∼150 meV, indicating that a weakly bound complex is formed. The mean distance between the two components is estimated to be around 10 Å, consistent with the effective charge-transfer distance.

Ionic screening of the complex formation puts a limit on the concentration of buffer that can be used in attempts to detect DNA fragments. Though a relatively high ion concentration is required for formation of the DNA double helix, complex formation at this high concentration is inhibited. Thus, the fluorescence quenching/unquenching cannot be used in its simplest conceptual form for recognition of DNA.

In addition to the static quenching mode studied in the buffer solution, the upward curvature in the Stern−Volmer plots shows the existence of a sphere-of-action quenching. To properly describe the combination of the two quenching mechanisms, a modified Stern−Volmer equation is used to fit the data. The radius (∼400 Å) of the sphere-of-action is then derived from the data. The static mode and the sphere-of-action effects compete against each other on the fluorescence quenching at high temperature. A drop in the relative increase of PL at high temperature in the high concentration MV^{2+} solution shows the crossover of the quenching from the static mode to the sphere-of-action mode. A sphere-of-action with the same size is obtained from the crossover point, comparable to the size of the polymer chain. Thus, the large size of the polymer chain enhances the quenching and thus enhances the potential sensitivity in biosensing applications.

Acknowledgment. This research was supported by the National Science Foundation (DMR9730126) and by a subcontract from the Los Alamos National Laboratory (DOE subcontract J0223). We thank Dr. D. McBranch and Dr. D. Whitten (QTL Biosystems), Dr. Peter Heeger (Case Western Reserve University), and Dr. Jian Pei (National University of Singapore) for many useful discussions.

References and Notes

(1) (a) Burroughes, J. H.; Bradley, D. D. C.; Brown, A. R.; Marks, R. N.; Mackay, K.; Friend, R. H.; Burns, P. L.; Holmes, A. B. *Nature* **1990**, *347*, 539. (b) Braun, D.; Heeger, A. J. *Appl. Phys. Lett.* **1991**, *58*, 1982. (c) Zhang, C.; Braun, D.; Heeger, A. J. *J. Appl. Phys.* **1993**, *73*, 5177. (d) Parker, I. D. *J. Appl. Phys.* **1994**, *75*, 165.

(2) (a) Pei, Q.; Yu, G.; Zhang, C.; Yang, Y.; Heeger, A. J. *Science* **1995**, *269*, 1086. (b) Cao, Y.; Yu, G.; Heeger, A. J.; Yang, C. Y. *Appl. Phys. Lett.* **1996**, *68*, 3218. (c) Gao, J.; Yu, G.; Heeger, A. J. *Appl. Phys. Lett.* **1997**, *71*, 1293.

(3) (a) Moses, D. *Appl. Phys. Lett.* **1992**, *60*, 3215. (b) Hide, F.; Diaz-Garcia, M. A.; Schwartz, B. J.; Andersson, M. R.; Pei, Q.; Heeger, A. J. *Science* **1996**, *273*, 1833. (c) McGehee, M. D.; Diaz-Garcia, M. A.; Hide, F.; Gupta, R.; Miller, E. K.; Moses, D.; Heeger, A. J. *Appl. Phys. Lett.* **1998**, *72*, 1536.

(4) Yu, G.; Gao, J.; Hummelen, J.; Wudl, F.; Heeger, A. J. *Science* **1995**, *270*, 1789.

(5) Yu, G.; Wang, J.; McElvain, J.; Heeger, A. J. *Adv. Mater.* **1998**, *17*, 1431.

(6) Chen, L.; McBranch, D. W.; Wang, H.; Helgeson, R.; Wudl, F.; Whitten, D. *Proc. Natl. Acad. Sci. U.S.A.* **1999**, *96*, 12287.

(7) Hide, F.; Ciaz-Garcia, M. A.; Schwartz, B. J.; Heeger, A. J. *Acc. Chem. Res.* **1997**, *30*, 430.

(8) Heeger, P. S.; Heeger, A. J. *Proc. Natl. Acad. Sci. U.S.A.* **1999**, *96*, 12219.

(9) Shi, S.; Wudl, F. *Macromolecules* **1990**, *23*, 2119.

(10) Israelachvili, J. In *Intermolecular & Surface Forces*, 2nd ed.; Academic Press Inc.: San Diego, 1991.

(11) Pesce, A. J. In *Fluorescence Spectroscopy*; Pesce, A. J., Rosén, C. G., Pasby, T. L., Eds.; Marcel Dekker Inc.: New York, 1971.

(12) Lakowicz, J. R. In *Principles of Fluorescence Spectroscopy*, 1st ed.; Plenum Press: New York, 1983.

(13) Frank, I. M.; Vavilov, S. I. *Z. Phys. Chem. (Munich)* **1931**, *69*, 100.

(14) Wang, D.; Wang, J.; Moses, D.; Bazan, G. C.; Heeger, A. J. To be published.

(15) Eftink, M. R.; Bhiron, C. A. *Anal. Biochem.* **1981**, *114*, 199.

(16) Flory, P. J. In *Principles of Polymer Chemistry*; Cornell University Press: Ithaca, NY, 1953.

(17) (a) Frank, I. M.; Vavilov, S. I. *Z. Phys.* **1931**, *69*, 100. (b) Moon, A. Y.; Poland, D. C.; Scheraga, H. A. *J. Phys. Chem.* **1965**, *69*, 2960. (c) Lakowicz, J. R.; Weber, G. *Biochemistry* **1973**, *12*, 4161.

(18) (a) Eftink, M. R.; Ghiron, C. A. *J. Phys. Chem.* **1976**, *80*, 486. (b) Andre, J. C.; Niclause, M.; Ware, W. R. *Chem. Phys.* **1978**, *28*, 371.

MA000081J